High-Resolution Structures of the Amyloid-β 1-42 Dimers from the Comparison of Four Atomistic Force Fields

Viet Hoang Man,[1] Phuong H. Nguyen,[2] Philippe Derreumaux[2*]

[1] Department of Physics, North Carolina State University, Raleigh, NC 27695 - 8202, USA
[2] Laboratoire de Biochimie Théorique, UPR 9080 CNRS, Université Paris Diderot, Sorbonne Paris Cité, IBPC, 13 Rue Pierre et Marie Curie, 75005 Paris, France

Supporting Information

System	State	P	$(\beta,\alpha)_a$	$(\beta,\alpha)_b$	$(\beta,\alpha)_c$	N_1	N_2	N_3	Res$_\alpha$	Res$_\beta$
F14	1	13.32	(6, 14)	(1, 71)	(8, 43)	5	5	4	24-26,28-36	
	2	12.54	(10,7)	(2, 60)	(21,16)	5	5	4	28-34	
	3	12.08	(3, 8)	(70, 0)	(59, 1)	5	11	3	3-7,	17-22,29-33,36-39
	4	11.75	(10, 10)	(0, 81)	(1, 64)	5	7	4	2-4,14-24,28-35	
	5	10.97	(8, 14)	(1, 56)	(29, 6)	4	4	3	13-15	
	6	10.68	(5, 14)	(15,52)	(51, 3)	5	7	3	14-20	21 -27, 30-36
	7	9.86	(13, 1)	(20, 0)	(29,16)	5	11	5	34-36	
	8	6.31	(15, 2)	(7, 6)	(24,12)	5	5	6		
	9	6.25	(5, 7)	(3, 32)	(3, 58)	6	6	3	28-37	
	10	6.25	(8, 13)	(17,13)	(22, 4)	5	6	5	7-17,	20-22,29-31
F22	1	12.55	(9, 11)	(3, 22)	(11, 41	4	4	3	19-27	
	2	12.43	(9, 6)	(28, 5)	(30, 9)	4	5	2		
	3	12.13	(11, 10)	(3, 47)	(23, 10)	4	5	3	17-19,31-34	
	4	11.73	(11, 9)	(1, 62)	(8, 38)	4	5	4	17-19,28-36	
	5	9.77	(12, 4)	(14, 4)	(16, 36)	3	6	2	30-34,36-38	
	6	9.58	(10, 13)	(1, 62)	(2, 63)	4	5	3	17-27,31-36	
	7	9.50	(10, 7)	(10, 18)	(30, 8)	4	5	3	4-6,	
	8	8.50	(15, 4)	(41, 1)	(47, 2)	5	8	3		
	9	7.92	(12, 4)	(15, 8)	(4, 64)	4	4	2	8-10,22-26, 31-36	
	10	5.90	(10, 8)	(10, 20)	(35, 1)	5	6	3	18-20,22-28,	31-32,39-41
F99	1	15.75	(21, 3)	(24, 2)	(38, 1)	4	6	3	24-27	
	2	15.37	(15, 4)	(49, 0)	(46, 1)	4	8	4		4-6,10-12,22-24,27-29
	3	15.02	(20, 2)	(27, 2)	(37, 5)	4	6	4	31-33	4-6,9-11
	4	11.20	(17, 3)	(22, 4)	(26, 10)	4	6	3	33-35	17-20, 30-32
	5	9.95	(21, 6)	(9, 14)	(35, 5)	4	4	4	9-11,15-17	
	6	8.53	(25, 4)	(57, 0)	(58, 0)	6	8	2	9-11	30-32,38-40
	7	7.68	(24, 6)	(4, 13)	(10, 36)	4	4	5	28-36	
	8	5.96	(6, 9)	(13, 34)	(56, 2)	5	7	3	17-19	10-12,21-27,30-36
	9	5.35	(26, 9)	(17, 24)	(38, 2)	5	5	4	13-17,	22-23, 26-27
	10	5.18	(11, 4)	(74, 0)	(60, 1)	3	9	3		19-22, 29-32, 36-37
FOP	1	17.62	(15, 2)	(21, 1)	(40, 0)	4	7	5		
	2	16.52	(10, 2)	(40, 1)	(41, 0)	4	9	5	16-20,31-36	
	3	14.73	(14, 2)	(17, 3)	(26, 1)	5	5	4	14-16	
	4	10.05	(10, 7)	(21, 31)	(55, 0)	6	9	3		21-27,30-36
	5	9.61	(11, 6)	(12, 13)	(42, 0)	5	4	3		29-31, 38-40
	6	7.87	(16, 5)	(2, 30)	(27, 1)	6	5	3		3-6,10-14
	7	7.59	(16, 2)	(5, 13)	(16, 8)	6	4	5		11-12, 35-36
	8	6.27	(19, 3)	(52, 0)	(52, 0)	5	11	3		3-9,14-20, 31-37
	9	5.06	(8, 6)	(6, 28)	(31, 0)	7	4	3	17-20	
	10	4.67	(6, 7)	(10, 25)	(41, 0)	8	9	3		

TABLE S1: Characterization of 10 single states of the Aβ_{42} dimers . Shown are the population P (in %), the average value of two secondary structures $(\beta,\alpha)_{a,b,c}$ pertained to Nter (a), CHC (b), CHC (c) regions, the average value of the intramolecular contacts between Nter-CHC (N_1), Cter-CHC (N_2), Nter-Cter (N_3), and the positions of the residues forming helical (Res$_\alpha$) and β (Res$_\beta$) segments.

FF	State	P	β	α	turn	N_1	N_2	N_3	N_4	N_5	CCS	FF	State	P	β	α	turn	N_1	N_2	N_3	N_4	N_5	CCS
F14	1	8.30	21	12	37	2	8	3	2	3	1246	F99	1	3.03	14	7	43	5	5	3	2	15	1272
	2	4.88	22	5	36	2	8	3	9	5	1210		2	3.00	21	5	50	2	7	2	6	18	1212
	3	4.12	7	31	28	3	5	4	0	18	1158		3	2.61	18	14	39	2	0	1	18	4	1248
	4	4.09	18	17	40	2	5	0	12	11	1279		4	2.57	35	1	36	2	7	5	18	2	1328
	5	3.07	20	9	41	3	14	4	4	12	1323		5	1.92	38	1	41	4	1	1	2	3	1262
	6	2.68	23	6	42	5	7	4	17	12	1245		6	1.88	36	1	36	4	5	3	2	1	1383
	7	2.45	10	22	39	6	2	3	9	15	1251		7	1.74	26	4	38	7	7	4	6	6	1410
	8	2.37	0	41	36	3	9	1	1	2	1220		8	1.58	22	13	37	3	5	1	0	0	1278
	9	2.32	5	28	41	2	14	1	3	0	1243		9	1.51	29	1	42	2	5	8	9	4	1275
	10	2.14	18	19	33	1	1	0	8	12	1316		10	1.47	20	1	46	6	4	5	0	10	1190
F22	1	2.65	6	24	43	6	3	5	5	0	1228	FOP	1	4.49	28	5	43	3	7	0	3	4	1266
	2	2.21	18	32	28	1	14	1	0	11	1176		2	3.68	19	1	52	6	1	6	0	13	1173
	3	2.11	8	28	40	5	4	1	14	0	1301		3	3.08	25	2	48	2	12	7	4	8	1274
	4	1.81	5	21	40	4	9	3	11	19	1224		4	3.03	43	0	31	2	9	0	1	16	1310
	5	1.68	10	24	46	8	9	4	4	16	1214		5	2.95	19	6	47	6	4	2	16	3	1263
	6	1.47	6	26	46	2	4	3	9	18	1409		6	2.83	15	4	48	3	8	5	2	4	1292
	7	1.40	21	9	43	1	13	1	7	16	1400		7	2.81	20	2	52	4	0	0	5	9	1243
	8	1.23	12	19	44	2	11	0	5	8	1294		8	2.72	21	3	46	4	8	3	5	13	1220
	9	1.20	20	13	45	0	17	0	4	16	1301		9	2.60	17	3	42	4	10	0	5	9	1288
	10	1.15	18	9	48	7	7	2	11	13	13017		10	2.60	17	5	46	9	4	1	21	4	1268

TABLE S2: Characterization of the first 10 overall states (S_k) of the Aβ_{42} dimer obtained by 4 force fields. Shown are the population P (in %), the average values of various secondary structure contents (in %), the average Q values of intermolecular contacts between Nter-CHC (N_1), Cter-CHC (N_2), Nter-Nter (N_3), CHC-CHC (N_4) and Cter-Cter (N_5). The CCS value of each representative structure is also shown. The combination of the single-molecular states (s_i, s_j) that form the overall states S_k are: F14: $S_1 = (s_8, s_1)$, $S_2 = (s_{10}, s_8)$, $S_3 = (s_9, s_4)$, $S_4 = (s_{10}, s_2)$, $S_5 = (s_{10}, s_9)$, $S_6 = (s_{10}, s_7)$, $S_7 = (s_5, s_4)$, $S_8 = (s_6, s_4)$, $S_9 = (s_6, s_5)$, $S_{10} = (s_4, s_1)$. F22: $S_1 = (s_9, s_6)$, $S_2 = (s_{10}, s_3)$, $S_3 = (s_9, s_1)$, $S_4 = (s_{10}, s_3)$, $S_5 = (s_8, s_8)$, $S_6 = (s_{10}, s_6)$, $S_7 = (s_7, s_7)$, $S_8 = (s_6, s_4)$, $S_9 = (s_7, s_5)$, $S_{10} = (s_7, s_5)$. F99: $S_1 = (s_5, s_3)$, $S_2 = (s_6, s_5)$, $S_3 = (s_6, s_4)$, $S_4 = (s_7, s_5)$, $S_5 = (s_{10}, s_2)$, $S_6 = (s_8, s_2)$, $S_7 = (s_{10}, s_4)$, $S_8 = (s_9, s_1)$, $S_9 = (s_8, s_7)$, $S_{10} = (s_{10}, s_3)$. FOP: $S_1 = (s_{10}, s_8)$, $S_2 = (s_{10}, s_{10})$, $S_3 = (s_9, s_4)$, $S_4 = (s_9, s_4)$, $S_5 = (s_8, s_6)$, $S_6 = (s_7, s_5)$, $S_7 = (s_{10}, s_6)$, $S_8 = (s_{10}, s_1)$, $S_9 = (s_9, s_6)$, $S_{10} = (s_8, s_7)$.
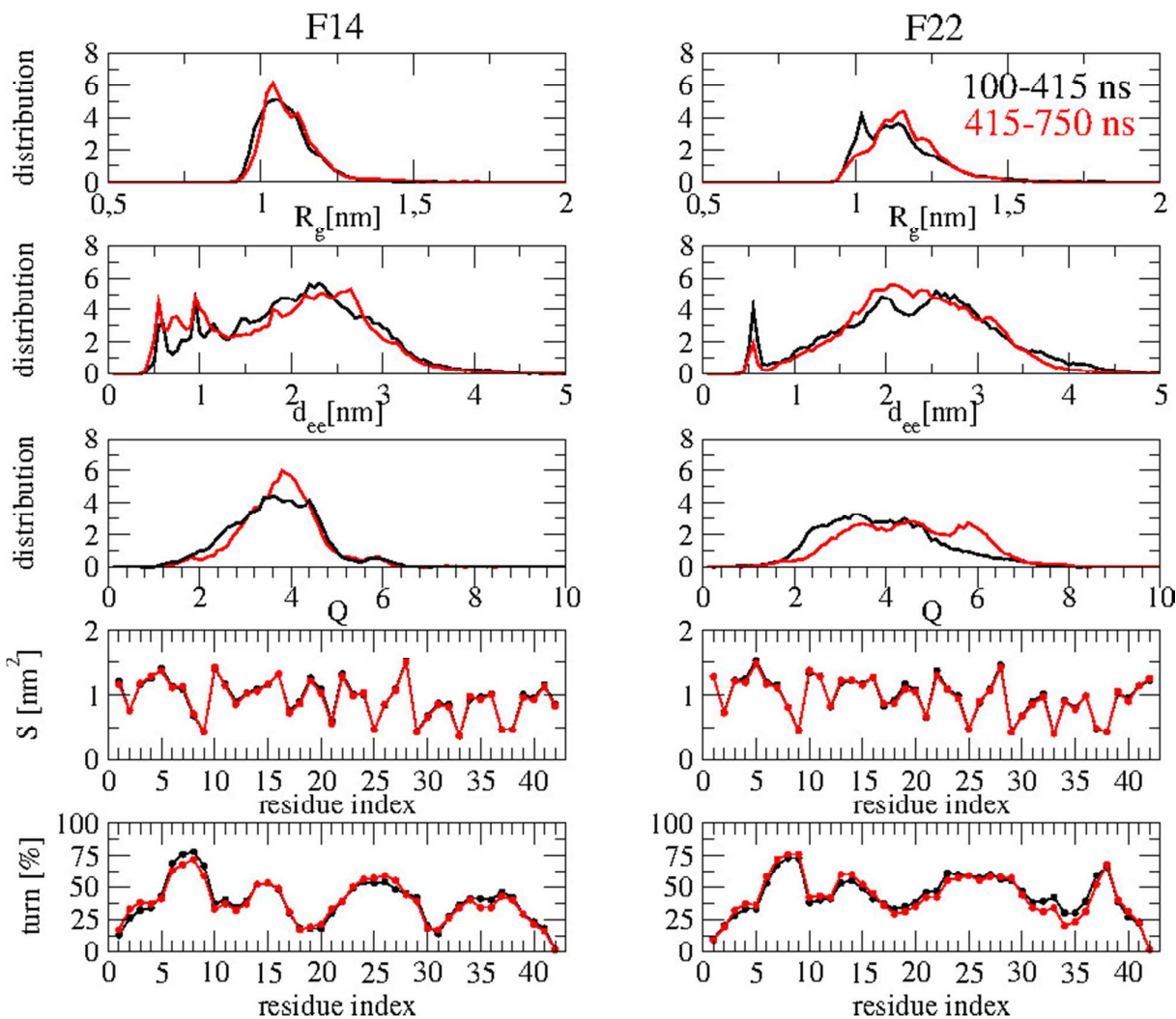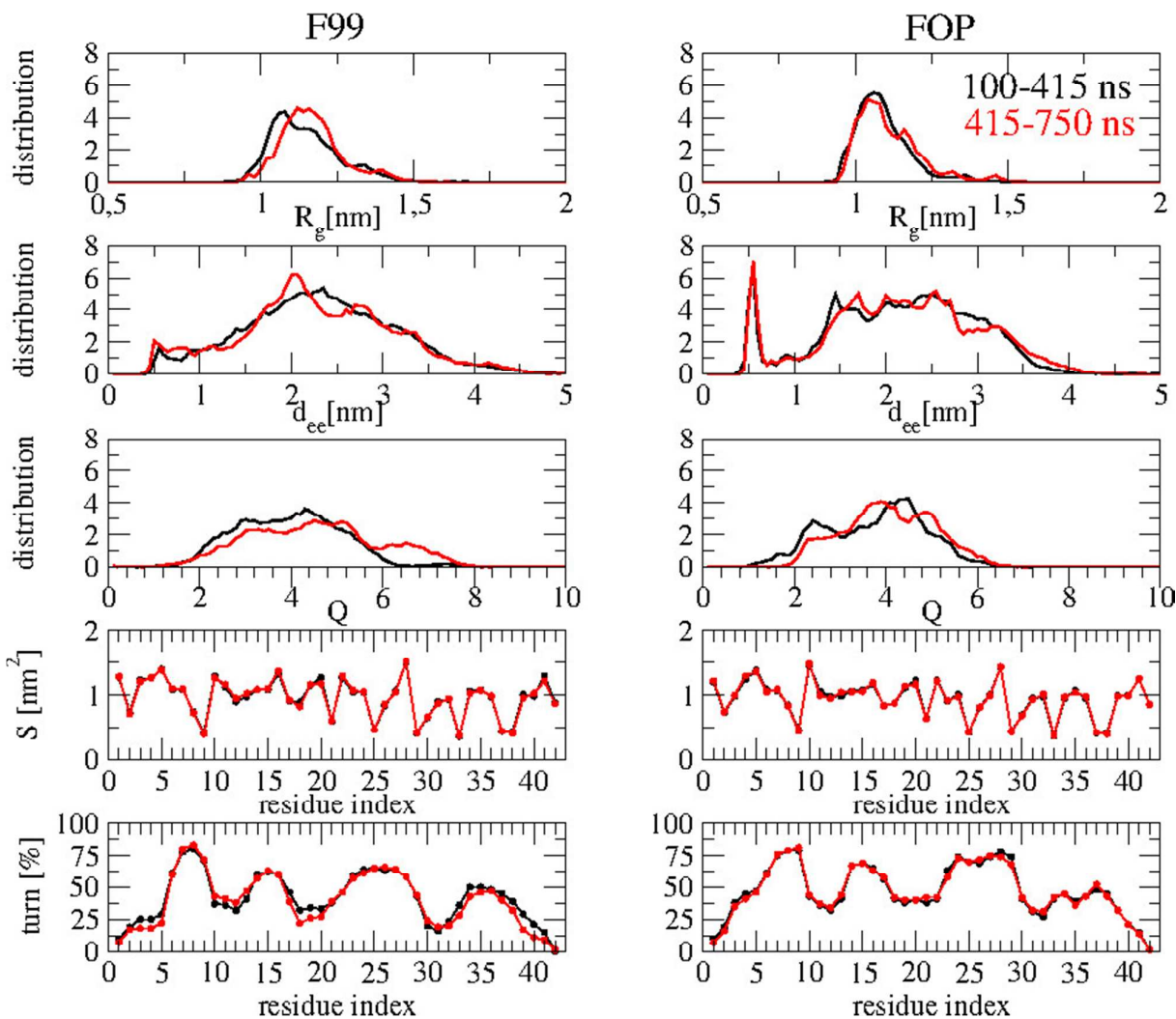
Figure S1. Convergence of REMD simulations with the F14 and F22 force fields at 315 K. Shown are the distributions of various quantities including the radius of gyration (R_g), the Cα end-to-end distance (d_{ee}), the total number of intermolecular side-chain--side-chain contacts (Q), as well as the solvent accessible surface area (S) and the turn propensity of each residue. The results are calculated for two time intervals 100-415 ns (black curves) and 415-750 ns (red curves). The left and right panels display the results of the F14 and F22 force fields, respectively.

Figure S2. Convergence of the REMD simulations with the F99 and FOP force fields at 315 K. Shown are the distributions of various quantities including the radius of gyration (R_g), the $C\alpha$ end-to-end distance (d_{ee}), the total number of intermolecular side-chain--side-chain contacts (Q), as well as the solvent accessible surface area (S) and the turn propensity of each residue. The results are calculated for two time intervals 100-415 ns (black curves) and 415-750 ns (red curves). The left and right panels display the results of the F99 and FOP force fields, respectively.
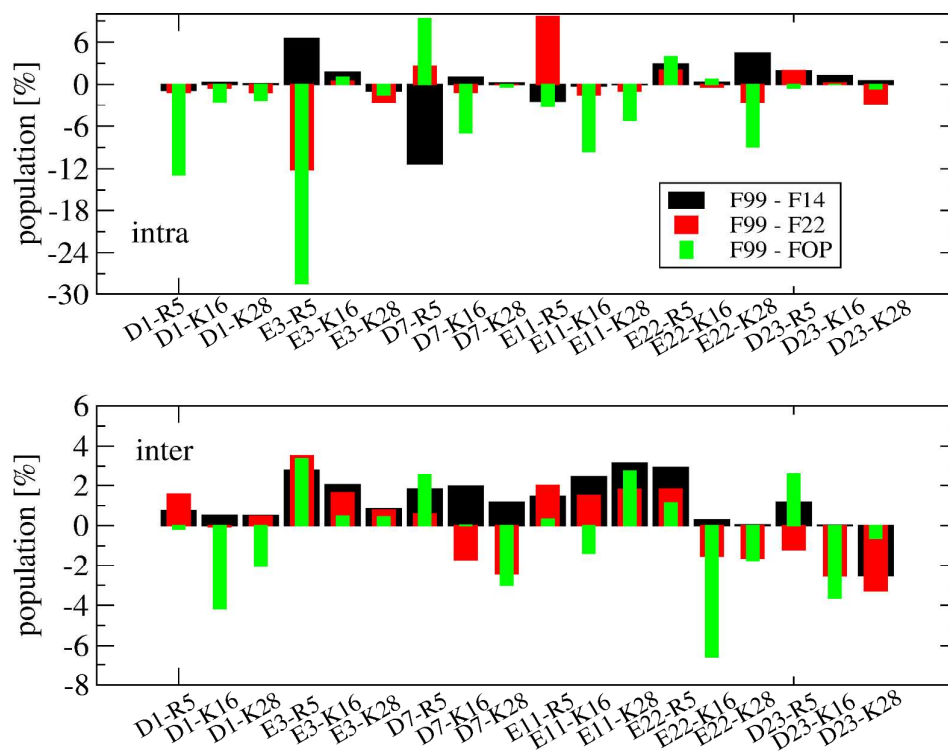
Figure S3. Differences in the populations (in %) of intramolecular (upper) and intermolecular salt bridges formed in Aβ42 dimer obtained from F14 (black), F22 (red), FOP (green) with respect to F99. The salt bridge distances are calculated between the atoms CG (in ASP1, ASP7, ASN7 or ASP23) or CD (in GLU3, GLU11, or GLU22) and the atom NH2 (in ARG5) or NZ (in LYS16 or LYS28). The cutoff distance used for considering one salt bridge formed is 0.46 nm. The error bars are at most of 3% using two independent time windows.
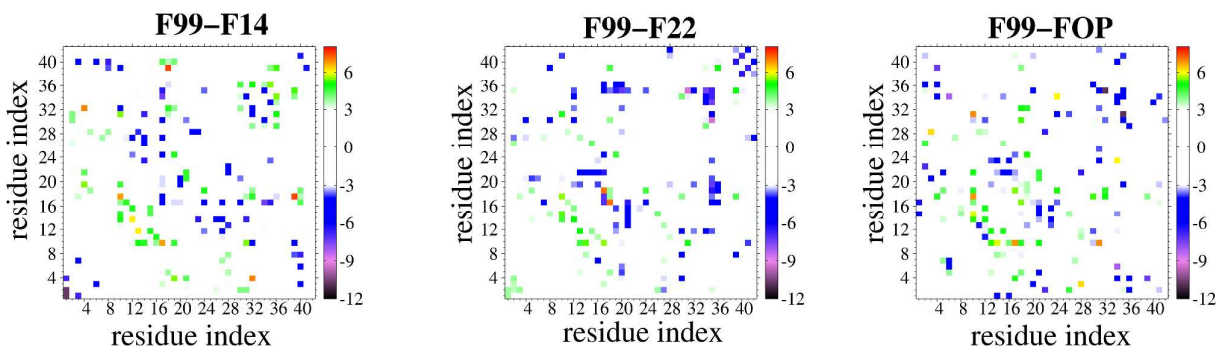
Figure S4. Differences of the inter-peptide side-chain – side-chain contact probabilities between F99 and the other force fields. F99-F14 (left), F99-F22 (middle) and F99-FOP (right). Only probability differences > ±3% are shown.
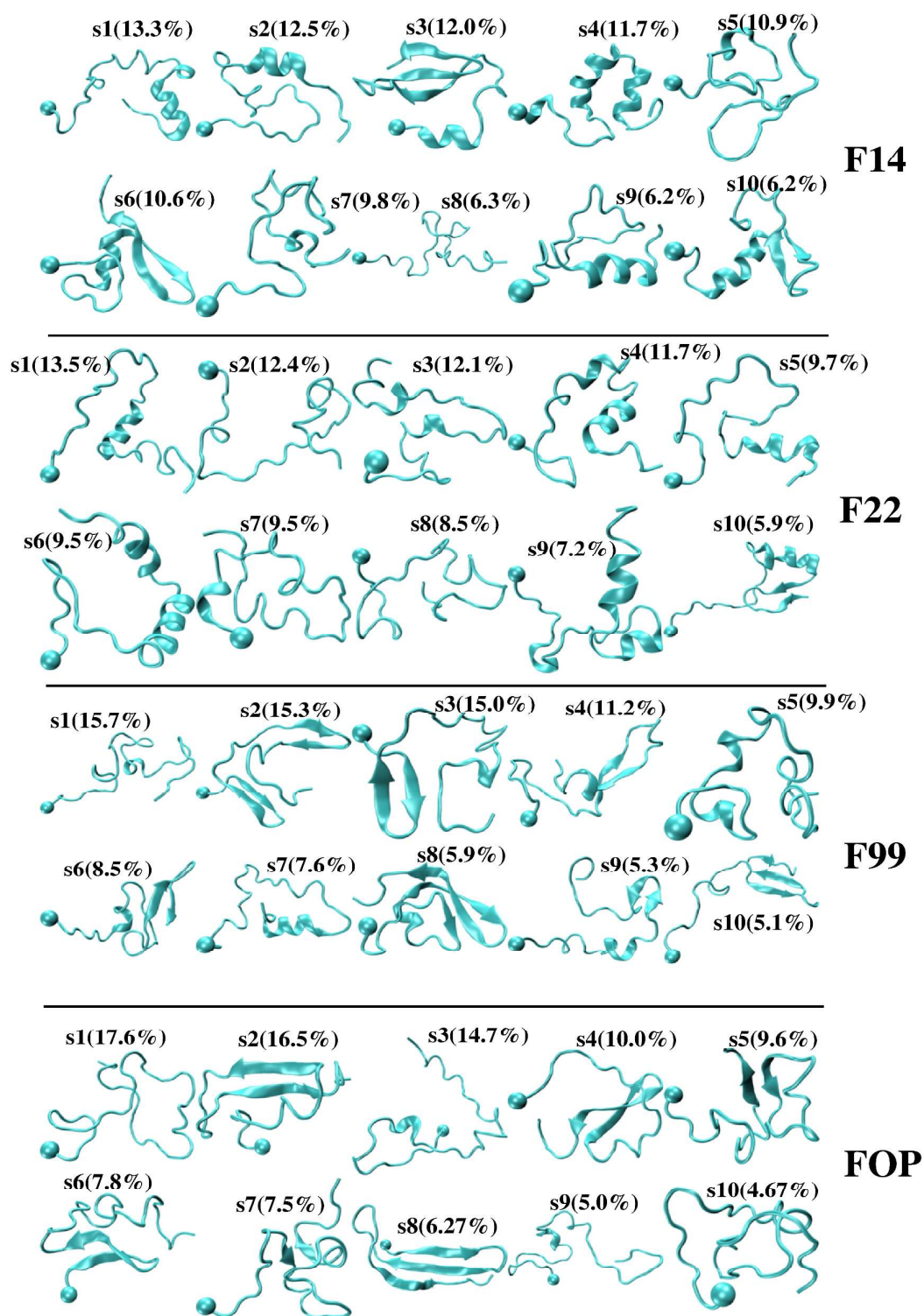
Figure S5. Representative structures of the 10 single-molecule states of Aβ42 dimer obtained using the four force fields. The ball indicates the first residue. The populations of the 10 states, s1-s10, are given.